RESEARCH PAPER

Hot Deformation of the Mn-Ni-Cr Alloy During Compression

M. Sadeghi[1], M. Hadi[2,*], O. Bayat[3] and H. Karimi[1]

** morteza.hadi@gmail.com*

Received: June 2019 **Revised: September 2019** **Accepted: December 2019**

[1] Materials Engineering Department, Malek Ashtar University of Technology, Iran.

[2] Metallurgy and Materials Engineering Department, Golpayegan University of Technology, Golpayegan, Iran.

[3] Department of Materials science and Engineering, Hamedan University of Technology, Hamedan, Iran.

DOI: 10.22068/ijmse.17.1.102

Abstract: *In this paper a constitutive equation was considered for isothermal hot compression test of the Mn-Ni-Cr alloy. Hot compression test was performed in strain rate range of 0.001-0.1 s^{-1} while deformation temperature was varied from 700 to 900 °C. A considerable reduction in flow stress was observed regardless of the strain rate when temperature raised from 700 to 750 °C. DTA and XRD evaluation revealed that removal of Mn_3Cr phase and formation of the single solid solution phase was the cause of the flow stress reduction. At low deformation temperature (700°C) and high strain rate (0.1 s^{-1}), a partially recrystallized microstructure was observed; so that with increasing the temperature and decreasing the strain rate, a recrystallized microstructure was completed. The relationships between flow stress, strain rate and deformation temperature were addressed by the Zener-Holloman parameter in the exponent type with the hot deformation activation energy of 301.07 KJ/mol. Finally, the constitutive equation was proposed for prediction of the flow stress at various strain rates and temperatures.*

Keywords: *Hot deformation, Constitutive equation, Zener-Holloman, Mn-Ni-Cr alloy.*

1. INTRODUCTION

There has been much research regrading Mn-Ni alloys owing to their magnetic properties [1-3]. It has been shown that the manganese- nickel alloys in the form of thin foils can be employed for the brazing of nickel-based superalloys and stainless steel. Manganese provides good compatibility with nickel- based superalloys; it also acts as an effective melting point depressant [4-5]. Mn-30Ni filler alloy has been utilized for the brazing of stainless steels [6]. As for the corrosion resistance, Dean et.al. has reported that these binary alloys have a tendency to tarnish rather quickly and to show premature evidence for general corrosion in the atmosphere as well as in an aqueous environments. Therefore, chromium is required to impart better resistance to atmospheric and general corrosion [4].

Brazing filler alloy is often used in very fine thickness (or diameter) in the form of foil (or wire). Therefore, deformation parameters particularly flow stress as a function of strain rate are very important in production process of brazing alloys. Arrhenius model has been applied for various alloying systems including Fe-Cr-Ni alloy [7], ultra-high strength steels [8], Al-Si alloy [9], Az24 magnesium alloy [10], AA785 aluminum alloy [11], and low carbon steel [12] to determine constitutive equation in order to predict flow stress. However, there is still a lack of experimental research focusing on the hot deformation behavior of Mn-Ni-Cr alloy. Hot compression behavior and its constitutive equation should therefore be considered to acquire an optimum temperature, strain rate and operation parameters of the hot rolling process, which are necessary to produce the filler brazing foil. Therefore, present investigation was carried out to determine a constitutive equation for the hot compression of the Mn-Ni-Cr alloy.

2. EXPERIMENTAL

Mn-25Ni-5Cr (%wt.) alloy was prepared by using Mn, Ni and Cr elements in a vacuum induction melting furnace under argon atmosphere. The cast ingots were homogenized at 950°C for 4 h. Cylindrical specimens with a diameter of 8

[Downloaded from idea.iust.ac.ir on 2026-11-09]

[DOI: 10.22068/ijmse.17.1.102]

mm and a height of 12 mm were machined from the ingots. To establish the stress- strain behavior of the alloy, uniaxial hot compression tests were conducted on a servo-hydraulic 500KN computerized material testing system equipped with a resistance furnace. The compression tests were performed in the temperature range of 700 - 900ºC, and the strain rate was varied from 0.001 to 0.1 S^{-1}. The samples were heated at a heating rate of 10ºC/min, and soaked for 10 min at the deformation temperature. The specimens were allowed to deform to half their original height and water quenched immediately. Fine grooves at the top and the end of specimens were machined to maintaini lubricant until the final stages of the test. Therefore, the effect of friction was well controlled and barreling in the specimens was approximately prevented. However, friction effect was removed using equation (1):

$$\sigma_a = \sigma_0 \left(1 + \frac{\mathrm{mD}}{3\sqrt{3}H}\right) \quad (1)$$

Where, σ_a, σ_0, and m represent measured axial stress, effective flow stress, and the friction coefficient, respectively. The barreling parameter of each specimen was calculated using equation (2) and the friction coefficient was measured with the help of standard tables.

$$B = \frac{h(r_{max})^2}{h_0(r_0)^2} \quad (2)$$

The deformed specimens were sectioned parallel to the compression axis for further analysis. The thermal transition behaviour was studied under non- isothermal condition using NETZCH STA 409 PC/PG differential thermal analyzer (DTA). Samples for microscopic examination were prepared using the standard metallographic procedures and were etched using 10ml H_2O+ 10ml HCL+ 1ml HNO3 solutions. As-cast and heat treated samples were characterized by utilizing the Philips x-ray diffractometer (XRD) with a Cu-Kα radiation at 30mA and 40 kV.

3. RESULTS AND DISCUSSION

The true stress-strain curves obtained at various deformation conditions are illustrated in Fig. 1. It can be seen that the influence of temperature and strain rate on flow stress is significant. It could also be observed that the true stress-strain curves have three distinct stages. In the initial stages of formation, the flow stress increases considerably as the strain enhances to a peak value, suggesting that the hard working rate is higher than the softening rate. Then the true stress-strain curves are gradually decreased or even kept constant with a variety of softening rates. However, it could be seen that the flow stress significantly decreases with increasing the temperature from 700 to 750 ˚C, suggesting a reduction in the strengthening mechanism of the alloy. The DTA graph of the alloy tested in the temperature range from room temperature to the melting point is shown in Fig. 2-(a). According to the Mn-Ni phase diagram (Fig. 2-(b)), the first and second peaks are related to the solid state transitions in the Mn-Ni phase system [13]. While the third one at 741ºC might be attributed to formation of a single solid solution phase called γ. To get further insight into this transformation, XRD analyses were performed. The XRD pattern of the specimen heat treated at 750 ˚C for 1 hour and then quenched into water was compared with that of the as-cast alloy (Fig. 3).

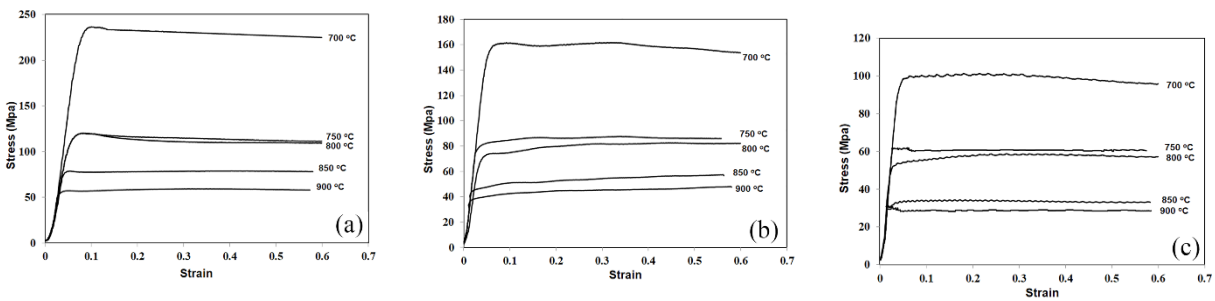

Fig. 1. The true stress-true strain curves of the alloy in the strain rate of (a) 0.1 s^{-1}, (b) 0.01 s^{-1}, and (c) 0.001 s^{-1}.

[Downloaded from idea.iust.ac.ir on 2026-11-09]

[DOI: 10.22068/ijmse.17.1.102]

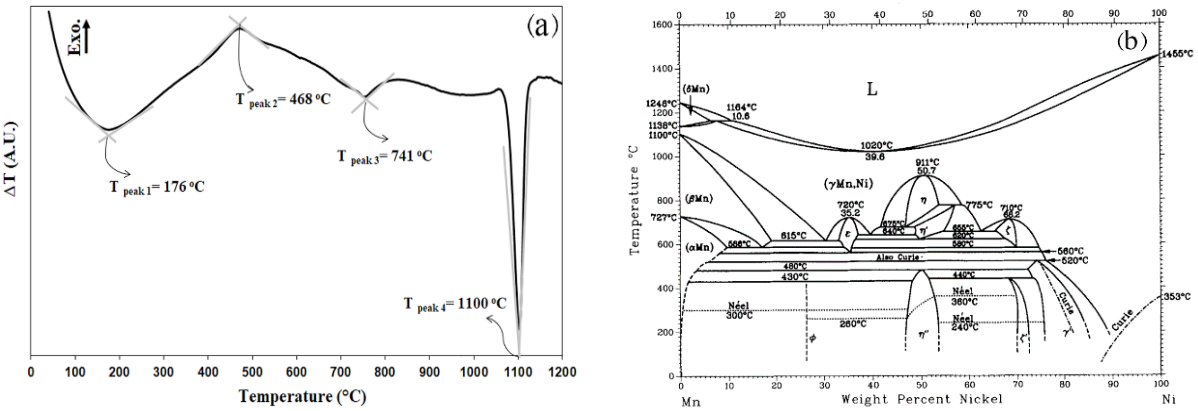

Fig. 2. (a) Thermo-analytical curve of the alloy from room temperature to melting point (b) Mn-Ni phase diagram [13].

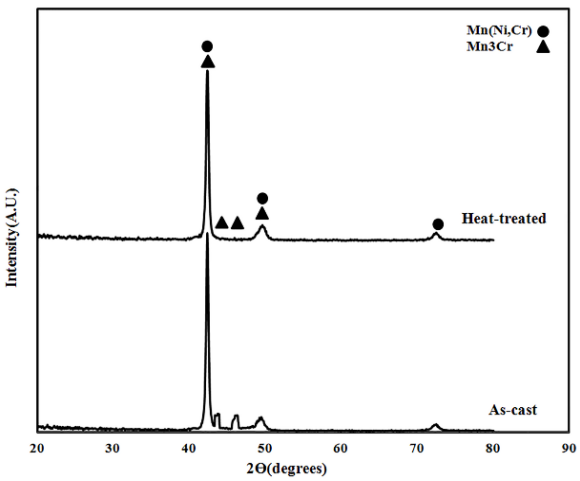

Fig. 3. The X-ray diffraction pattern of the Mn-25Ni-5Cr alloy.

γ-Mn (Cubic) and Mn_3Cr (Tetragonal) phases were identified in the as-cast pattern. However, the intensity of the Mn_3Cr peaks decrease (or approximately disappear) in the heat-treated specimen. Since the atomic radius of chromium (166 pm) is very close to that of manganese (161 pm), the peaks related to γ-solid solution does not show noticeable shift due to the solution of the remaining chromium atoms. Moreover, DTA and XRD results reveal that the first endothermic peak at 741 ˚C represents the dissolution of the Mn_3Cr and the formation of the single solid solution phase. Our previous study on another alloy system showed that the intermetallic compounds could have a strengthening effect on flow stress and a detrimental effect on ductility [14]. Accordingly, the formation of a single solid solution and the removal of intermetallic compounds from the microstructure might be regarded as a possible explanation for reduction in flow stress at temperatures higher than 741 ˚C. Meanwhile, by comparing this transition temperature with the Mn-Ni phase diagram [13], it could be concluded that the addition of chromium led to an increase in the solid solution temperature from ~ 625 ˚C for the Mn-30Ni alloy to ~741 ˚C for the Mn-25Ni-5Cr alloy. It should also be mentioned that the heating rate of DTA analysis and heat treatment was relatively low (10 ˚C/min); therefore, the reason for such a difference in transition temperature cannot be related only to the effect of the heating rate. It was found that the last endothermic peak which was related to the melting point of the alloy was shifted to the higher temperature (from ~1035 to 1100 ˚C) in the Mn-25Ni-5Cr alloy.

Another point arising from Fig. 1 is formation of a single peak in the flow curves. Generally, the flow stresses could be rapidly raised with the strain increase in the early stage of isothermal compressive deformation. This was undoubtedly be due to the domination of work hardening. It has been found that as the dislocation density increases, the effect of work hardening balances out with dynamic softening, with a peak appearing in the flow curve [14]. In fact, one of the characteristics of stress- strain curves under the DRX condition is the appearance of a peak diminishing flow stress and then stabilizing the flow stress. Nevertheless, the stress-strain curves were dropped slowly with an increase of the strain after the peak, suggesting that the DRX process for this alloy was rath-

[Downloaded from idea.iust.ac.ir on 2026-11-09]

[DOI: 10.22068/ijmse.17.1.102]

er sluggish. This could be attributed to the large amount of the alloying elements in this alloy which increases the SFE and therefore, promotes the recovery process. This type of behavior has also been observed in 904L austenitic stainless steel during the hot compression test [15]. Following the peak flow stress, the stress reached the steady state due to the balance between work hardening and flow softening. Meanwhile it could be seen from Fig.4 (a) that the microstructure of the hot deformed specimen at 700 ˚C and 0.1 s^{-1} contains both elongated (indicated by arrows) and equiaxed recrystallized grains indicating that partial dynamic recrystallization had occurred. However, no elongated grains were detected in the microstructure of the specimens deformed at 900 ˚C at the strain rate of 0.001 s^{-1} and the new grains formed by DRX could be clearly observed. Also, our results showed that while the microhardness of the specimen, deformed at 700 ºC and 0.1 s^{-1} with the elongated grains (fig. 4-a), was 280±10 H.V, it was 200±10 H.V. for the specimen deformed at 900 ºC and 0.001 s^{-1} with fully equiaxed microstructure. This evidence confirmed microstructural observations and suggested that while dynamic recovery and partial recrystallization had been occurred at low temperatures and high strain rates, DRX was the dominant softening process at high temperatures and low strain rates.

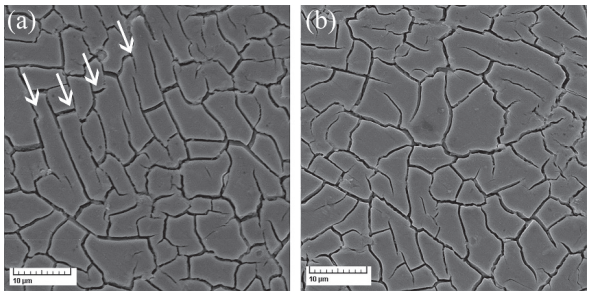

Fig. 4 - Microstructures of the Mn-25Ni-5Cr alloy deformed at different conditions, (a) 0.1 s^{-1} 700°C, and (b) 0.001 s^{-1} 900°C. Vertical dimension of the image are parallel to the compression axis.

On the other hand, from the flow curves it could be observed that the oscillation phenomenon had taken place at the low strain rate (0.001 s^{-1}). This is indicative of the fact that the alloy was completely recrystallized due to low strain rate and the high temperature. In a previous study done by the authors it was shown that higher temperature facilitates the formation of new grain boundaries and subsequently, low strain rate could provide the proper time for recrystallization [16-17]. Therefore, with the continuation of the deformation process, the alloy was hard worked, leading to a peak in the flow curves. Then, the softening process occurs and under these conditions, the amounts of flow stress oscillates during hot compression.

In order to further study the hot deformation behavior of the Mn-25Ni-5Cr alloy its deformation characteristics was investigated using a constitutive equation. Hot deformation of metallic materials is a thermal activation process and the strain rate is related to the temperature, the deformation activation energy, and the stress. Hot deformation is expressed by Arrhenius model as shown in the following equation [15]:

$$Z = \dot{\varepsilon} \, exp(Q/RT) = A[\sinh(\alpha\sigma)]^n \qquad (3)$$

Where, A is a constant, α is a temperature-independent material constant, n is a stress exponent, R is the universal gas constant, and Q is the activation energy for deformation. σ can be either peak stress or steady flow stress. In this paper, the steady flow stress was considered for calculation. It is generally accepted that the sine hyperbolic equation is suitable for constitutive analysis over a wide range of deformation temperature and strain rates [18-20].

To determine the constants by taking the natural logarithm from each side of the equation (3):

$$\ln(\dot{\varepsilon}) = \ln A + n\ln[\sinh(\alpha\sigma)] - Q/RT$$
$$n' = \left[\frac{\partial \ln \dot{\varepsilon}}{\partial \ln \sigma p}\right]_T$$
$$\beta = \frac{\partial \ln \dot{\varepsilon}}{\partial \sigma p}$$
$$n = \frac{\partial \ln \dot{\varepsilon}}{\partial \ln\{\sin(\alpha\sigma p)\}}$$

Where, n′ and β are the average slope of ln($\dot{\varepsilon}$) -σ and ln($\dot{\varepsilon}$)-ln(σ) lines at the constant temperature respectively. An approximate value of α was calculated by α= β/ n.

Fig. 5, Fig.6, and Fig.7 show β, n′, and n as obtained through the liner regression data; so the value of α is 0.01468. It is obvious that the lines at

[Downloaded from idea.iust.ac.ir on 2026-11-09]

[DOI: 10.22068/ijmse.17.1.102]

different temperatures are almost parallel; therefore, the correlation of the flow stress with the strain rate is slightly affected by temperature.

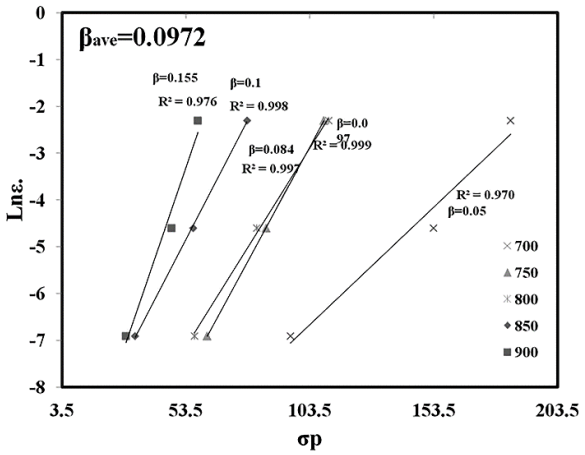

Fig. 5- The relationship between ln($\dot{\varepsilon}$)-σ.

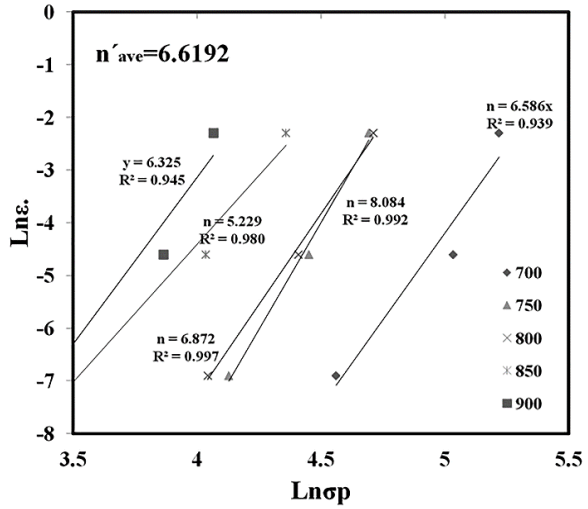

Fig. 6- The relationship between ln($\dot{\varepsilon}$)-ln(σ).

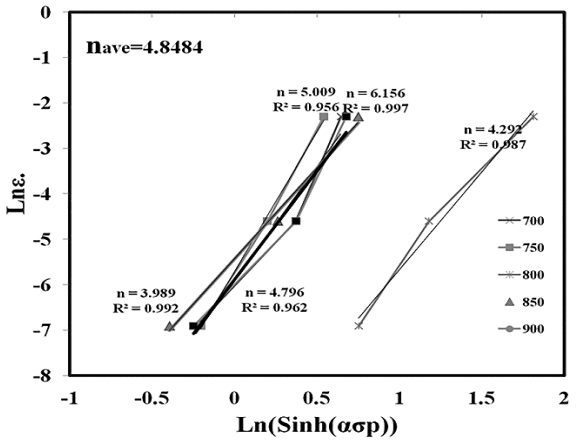

Fig. 7- The relationship between ln($\dot{\varepsilon}$)- ln[sinh(ασ)].

Rearranging Eq. (4) and differentiating with respect to 1/T result in an expression for the activation energy Q:

$$Q = \left[\partial \ln \dot{\varepsilon} / \partial \ln[\sinh(\alpha\sigma)]\right] T \left[\partial [\ln \sinh(\alpha\sigma)] / \partial(1/T)\right] \dot{\varepsilon} = RnS \quad (3)$$

Where S is the average slope of the lines in the ln[sinh(ασ)] against 1000/T plots, as shown in Fig. 8.

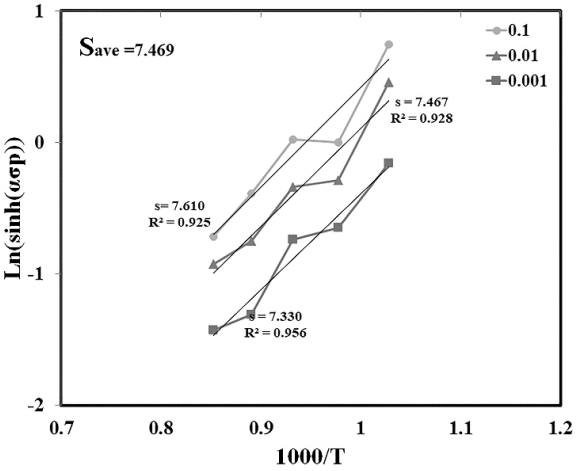

Fig. 8- The relationship between ln[sinh(ασ)]-1000/T.

The value of ln(A) is obtained from the intercept of the ln(Z) against ln[sinh(ασ)] plot, after calculation of the activation energy Q using Eq. (5). Generally, the hot deformation activation energy represents a difficulty in plasticity deformation. In the current study, Q is calculated to be 301.07 KJ/mol, which is higher than that for most conventional brass alloys [21] and lower than that for austenitic steel calculated by Pernis et.al [22]. It seems that the relatively high activation energy of the Mn-25Ni-5Cr alloy is the result of the high amounts of the solute alloying element in the Mn lattice.

On the other hand, the value of A could be calculated, as shown in Fig.9. To confirm the accuracy of the calculated parameters, the relationship between the measured peak stress (ln [sin h($_p$)]) and the Z parameter (ln(Z)) was plotted, as shown in Fig. 9. Regression analysis revealed that for this alloy, the correlation coefficient R is higher than 0.92; this indicates that the proposed constitutive equations could provide a reliable estimate of the flow stresses.

[Downloaded from idea.iust.ac.ir on 2026-11-09]

[DOI: 10.22068/ijmse.17.1.102]

$$\dot{\varepsilon} = 1.36203\times10^{12}\ [\ \sinh(0.01468\sigma)^{4.8484}]\exp(-\ 301072.4/RT) \quad (6)$$

$$\sigma = 1/0.0147Ln[(Z/1.36203 * 10^{12})^{1/4.84} + ((Z/1.36203 * 10^{12})^{2/4.84} + 1)^{1/2}] \quad (7)$$

Table 1. Values of material constants of Mn-Ni-Cr alloy

A(s^{-1})	α(Mpa^{-1})	n	Q(KJ/mol)
1.36203×10^{12}	0.0147	4.84	301.07

By substitution of the values in Table 1 in Eq. 3, we will get the isothermal compression equations of the alloy, as shown in Eqs. (6) and (7).

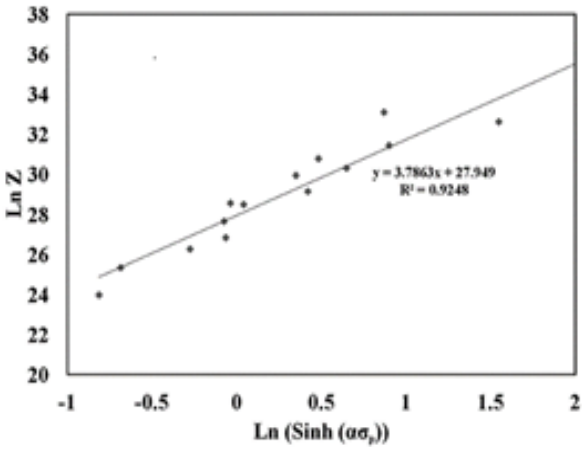

Fig. 9- The relationship between ln Z-ln[sinh(ασ)]

A good agreement between the predictions of the equation 5 and the obtained results for the examined conditions (the strain rate 0.001 to 0.1 s^{-1} and the temperature of 700 to 900 °C) signifies the applicability of the equations used for estimating flow stress at higher strain rates. On the basis of these obtained equations, the value of Z is desirable for the discussion of hot deformation in which T and ε^0 are known, whereas the flow stress is not measurable. According to the measured dissolution transition temperature (Fig. 2) and to reduce flow stress (Fig. 1), the temperature above 750 °C was selected for preheating in the actual rolling process of the alloy. Also, the strain rate was calculated according to the following equation applied in a similar research by Kratochvíl et.al. [23]:

$$\dot{\varepsilon} = 2/\sqrt{3}\ (\upsilon/\sqrt{R(H_0 - H_1)})\varepsilon_h \quad (8)$$

Where, H_0 and H_1 (mm) refer to the thickness of the specimen before and after rolling, ε_h is the true strain, υ (mm/s) is the peripheral velocity of the rolls, and R is the roll radius. The values of strain rate used in the equation 1 to calculate Z. Finally, the required stress for hot rolling was predicted by the equation 5. The observations of the actual hot rolling process of the alloy verifies that the maximum total reduction (MTR) up to 87% could be achieved by applying theses parameters.

4. CONCLUSIONS

In this study, the deformation of the Mn-25Ni-5Cr alloy was investigated at the deformation temperature of 700-900 °C and the strain rates of 0.001 to 0.1 s^{-1}. The following conclusions was drawn from the results obtained:

1. The flow stress of the alloy was affected by the temperature; the difference was particularly significant between 700 and 750 °C. The stress-strain curves, DTA and XRD results also showed that the flow stress of the alloy dramatically decreases at 750 °C due to the dissolution of Mn_3Cr phase and the formation of a single solid solution.
2. The stress-strain curves at low temperature and high strain rate were dropped slowly while the microstructure of the deformed specimens contained some remaining elongated grains. However, by increasing the temperature and decreasing the strain rate, dynamic recrystallization was clearly observed in the specimens. It is concluded that by reducing the value of the Z parameter, dynamic recrystallization could overcome the dynamic recovery.
3. The level of the flow stress of the Mn-25Ni-5Cr alloy could be described by a hyperbol-

[Downloaded from idea.iust.ac.ir on 2026-11-09]

[DOI: 10.22068/ijmse.17.1.102]

ic-sine constitutive equation with the deformation activation energy of 301.07 kJ/mol, and also by a Zener-Holloman parameter.

REFERENCES

1. Kasper, J. S. and Kouvel, J. S., "The antiferromagnetic structure of NiMn." Journal of Physics and Chemistry of Solids, 1959, 11, 231-238.
2. Nakamichi, T. and Yamamoto, M., "Composition, Temperature and Ordering Dependence of Magnetostriction Constants in Nickel-Manganese Alloys." Journal of the Physical Society of Japan, 1963, 18, 758-66.
3. Hicks, T. J., Pepper, A. R. and Smith, J. H., "Antiferromagnetism in γ-phase manganese-palladium and manganese-nickel alloys." Journal of Physics C: Solid State Physics, 1968, 1, 1683.
4. Dean, A. V. and Ennis, P. J., "Huntington Alloys Corp, assignee. Manganese-nickel alloys." US-patent, 1977, 4, 429.
5. Laux, B., Piegert, S. and Rösler, J., "Advancements in fast epitaxial high temperature brazing of single crystalline nickel based superalloys." In-Proceedings of the 11th International Symposium on Superalloys, 2008, 789-797.
6. Schwartz, M. M., "Source Book on Brazing and Brazing Technology." American Society for Metals, 1980, 428.
7. Zhou, L., Yang, L., Peng, Y., Fei, L. and Zhu, X., "Comparative study on constitutive models to predict flow stress of Fe-Cr-Ni preform reinforced Al-Si-Cu-Ni-Mg composite." Journal of Wuhan University of Technology-Mater. Sci. Ed, 2017, 32, 666-76.
8. Yang, X., Zhang, L., Shi, Y., Yu, S. and Hua, W., "Effect of niobium addition on hot deformation behaviors of medium carbon ultra-high strength steels." Journal of Wuhan University of Technology-Mater. Sci. Ed, 2017, 32, 162-72.
9. Huang, H. Q., Di, H. S., Yan, N., Zhang, J. C., Deng, Y. G., Misra, R. D. and Li, J. P., "Hot Deformation Behavior and Processing Maps of a High Al-low Si Transformation-Induced Plasticity Steel: Microstructural Evolution and Flow Stress Behavior." Acta Metallurgica Sinica, 2018, 31, 503-14.
10. Lai, L., Zhang, K., Ma, M., Li, X., Li, Y., Shi, G. and Yuan, J., "Hot deformation behavior of AZ40 magnesium alloy at elevated temperatures." Journal of Wuhan University of Technology-Mater. Sci, Ed. 2017, 32, 1470-5.
11. Liu, W., Zhao, H., Li, D., Zhang, Z., Huang, G. and Liu, Q., "Hot deformation behavior of AA7085 aluminum alloy during isothermal compression at elevated temperature." Materials Science and Engineering: A, 2014, 596, 176-182.
12. Liu, H., Liu, B., Li, D., Jin, X. and Zhang, Y., "Hot deformation behavior of low carbon steel during compression at elevated temperature." Journal of Wuhan University of Technology-Mater. Sci Ed, 2014, 29, 601-605.
13. Gokcen, N. A., "The Mn-Ni (manganese-nickel) system." Journal of phase equilibria, 1991, 12, 313-321.
14. Hadi, M. and Kamali, A. R., "Investigation on hot workability and mechanical properties of modified IC-221M alloy." Journal of Alloys and Compounds, 2009, 485, 204-8.
15. Humphreys, F. J. and Hatherley, M., "Recrystallization and related annealing phenomena" Elsevier. United Kingdom, 2004, 415-450.
16. Hadi, M., Meratian, M., Shafyei, A., "The effect of lanthanum on the microstructure and high temperature mechanical properties of a beta-solidifying TiAl alloy." Journal of Alloys and Compounds. 2015, 618, 27-32.
17. Hadi, M., Shafyei, A. and Meratian, M., "A comparative study of microstructure and high temperature mechanical properties of a β-stabilized TiAl alloy modified by lanthanum and erbium." Materials Science and Engineering: A, 2015, 624, 1-8.
18. Hu, H. E., Zhen, L., Yang, L., Shao, W. Z. and Zhang, B. Y., "Deformation behavior and microstructure evolution of 7050 aluminum alloy during high temperature deformation." Materials Science and Engineering: A, 2008, 488, 64-71.
19. Wei, G. Z., Lu, X., Ke, F. S., Huang, L., Li, J. T., Wang, Z. X., Zhou, Z. Y. and Sun, S. G., "Crystal habit-tuned nanoplate material of Li Li1/3–2x/3NixMn2/3–x/3. O2 for high-rate performance lithium-ion batteries." Advanced materials, 2010, 22, 4364-7.
20. Lin, Y. C. and Chen, X. M., "A critical review of experimental results and constitutive descriptions for metals and alloys in hot working." Materials & Design, 2011, 32, 1733-59.
21. Reyes-Calderón, F., Mejía, I. and Cabrera, J. M., "Hot deformation activation energy (QHW) of austenitic Fe–22Mn–1.5 Al–1.5 Si–0.4 C TWIP steels microalloyed with Nb, V, and Ti." Materials Science and Engineering: A, 2013, 562, 46-52.
22. Pernis, R., Kasala, J. and Boruta, J., "High temperature plastic deformation of CuZn30 brass–calculation of the activation energy." Kovové Materiály—Metallic Materials, 2010, 48, 41-6.
23. Kratochvíl, P. and Schindler, I., "Hot rolling of iron aluminide Fe28. 4Al4. 1Cr0. 02Ce (at %)." Intermetallics, 2007, 15, 436-8.

[Downloaded from idea.iust.ac.ir on 2026-11-09]

[DOI: 10.22068/ijmse.17.1.102]